ACS APPLIED MATERIALS & INTERFACES

Research Article

www.acsami.org

# Stronger and Faster Degradable Biobased Poly(propylene sebacate) as Shape Memory Polymer by Incorporating Boehmite Nanoplatelets

Wenshan Guo,[†] Hailan Kang,[‡] Yongwen Chen,[†] Baochun Guo,*[,†,§] and Liqun Zhang*[,‡]

[†]Department of Polymer Materials and Engineering, South China University of Technology, Guangzhou, 510640, P. R. China

[‡]Key Laboratory of Beijing City for Preparation and Processing of Novel Polymer Materials, Beijing University of Chemical Technology, Beijing, 100029, P. R. China

[§]State Key Laboratory of Pulp and Paper Engineering, South China University of Technology, Guangzhou, 510640, P. R. China

Supporting Information

**ABSTRACT:** Boehmite (BM) nanoplatelets were adopted to compound with fully biobased poly(propylene sebacate) (PPSe) to form the shape memory composites. The PPSe/BM composites kept excellent shape memory properties as previously reported PPSe. Compared to neat PPSe, the composites possess much higher mechanical properties above the melting point and faster biodegradation rate, which was demonstrated via tensile test at elevated temperature and in vitro degradation experiments in phosphate buffer saline (PBS), respectively. The obviously improved mechanical properties at elevated temperature are attributed to the uniform dispersion of the reinforcing boehmite nanoplatelets, which was facilitated by the interfacial interaction between BM and PPSe as revealed by FTIR, XPS, and XRD results. The faster degradation is correlated to accelerated hydrolysis by basic boehmite with surface aluminols. The potential biocompatibility, as substantiated by the outstanding cell viability and cell attachment, together with the realization of transformation temperature close to body temperature makes the PPSe/BM composites suitable for the biomedical applications, such as stents, in human body.

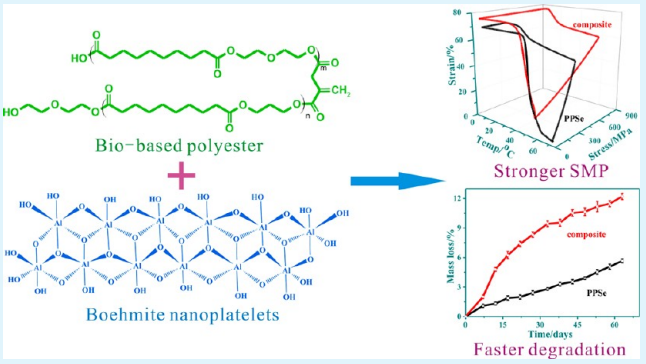


**KEYWORDS:** *shape memory polymer, biobased polyester, degradability, boehmite*

## INTRODUCTION

Shape memory polymers (SMPs) have sensitive response to external stimuli, such as temperature,[1] light,[2] humidity,[3] electricity,[4] magnetic field,[5] and so on. Until now, the majority of the reported SMPs are stimulated by temperature. Although SMPs have many advantages over shape memory alloys, like low density, large deformability, easy processability, and low cost,[6] some of the major drawbacks of SMPs strongly limit their applications, such as poor mechanical properties, low recovery stress, slow recovery speed, and low degradation rate, etc.[7] For example, for some special biomedical applications of shape memory polymers, such as hard tissue implantations and short-term clinical outcomes, high strength and fast degradation rate are desired, respectively.[8,9] To meet broader and stricter performance needs of SMPs, different types of reinforcements including carbonaceous materials and inorganics have been introduced to modify their electrical properties, thermal properties, mechanical properties, and biodegradability.

By incorporating carbonaceous fillers such as carbon nanotubes (CNTs), resistive heating,[10] electric,[11] infrared radiation,[12] or laser[13] triggered shape memory behaviors of polymers could be achieved for actuators or medical applications. For example, Cho et al.[14] prepared a series of shape-memory polyurethane composites incorporating CNTs. The electrical conductivity of the composites was greatly improved, realizing shape-memory behavior actuated by applying a voltage. In addition, the mechanical properties of the composites were also enhanced. When a voltage of 30 V was applied to a PU-SWCNT hybrid containing 4% of SWCNTs at 5 °C, a good shape recovery of 88% in 90 s occurred.[15]

Recently, biodegradable SMPs have been explored as an alternative to biodegradable implants because no material remains in the body after they serve their functions, with degradation through either hydrolytic or enzymatic breaking down of constituent bonding.[16−19] The biodegradability of the SMPs could be changed via introducing inorganic fillers. Via introducing hydrophilic $Fe_3O_4$ nanoparticles, poly(ε-caprolactone)(c-PCL) degraded faster in PBS, and the degradation rate increased with incremental $Fe_3O_4$ content.[20] Nevertheless, the shape recovery ratio of the PCL/$Fe_3O_4$ composites decreased compared to pure PCL. Although the

Received: May 11, 2012
Accepted: July 16, 2012
Published: July 20, 2012

  

poly(D,L-lactide) (PDLLA)/hydroxyapatite (HA) composites showed much improved shape-memory properties compared with neat PDLLA, the degradation rate was found to be depressed.[21,22] Mather et al.[23] studied biodegradable poly(lactide-co-glycolide) (PLGA) oligomers which incorporated polyhedral oligosilsesquioxane (POSS) as the center to synthesize a organic−inorganic hybrid. The networks exhibited versatile shape memory properties, however, with increasing POSS content, the crystallinity of the network increased and the degradation rate decreased.

Meanwhile, the energy, resources and serious environmental problems influence our life deeply today. The full use of renewable resources and the reducing dependence on fossil fuels have been paid global attention to by many scientists. Consequently, the SMPs derived from biomasses or their extracts are of great importance and highly desired. However, most of the reported biobased SMPs showed inferior mechanical properties,[24] which limited their applications as some kinds of biomedical materials or devices. In such circumstances, it is essential to improve their mechanical properties, including the strength and the rubbery modulus of the polymer networks,[7,25] so that we can get SMPs with more excellent shape memory properties.

Previously, we synthesized a series of biobased SMPs with biodegradability and biocompability.[26] However, the SMPs also have some defects like most biobased polyesters, such as low mechanical properties, especially above melting point ($T_m$), and unsatisfying degradation rate. In the present work, poly(propylene sebacate) (PPSe) with cross-linkable pendent groups was synthesized fully using biobased raw materials including 1,3-propanediol (PDO), sebacic acid (SA), and itaconic acid (IA). BM nanoplatelets have a typical layered lamella structure with only one kind of basic unit of AlO(OH).[27−29] The nanoplatelets consist of $AlO_6$ octahedron units and have abundant surface aluminols, which endow BM surface basicity.[30] Compared to the surface basicity of BM, montmorillonite clay with both surface aluminols and silanols, were Lewis acidic.[31] In the present work, the strong interfacial interaction between BM and polyster and faster degradation properties of the polyester/BM composites are related to the basic surface of BM. In our research, BM was introduced to improve the mechanical properties above $T_m$ and accelerate the biodegradation rate of PPSe, making SMPs of PPSe/BM composites potential candidates in kinds of biomaterials, such as high strength stents, hard tissue implantations or short-term clinical outcomes in which fast degradation is necessary. The high temperature dynamic modulus was enhanced as well. PPSe maintained excellent shape memory properties when BM was loaded. And the transformation temperature of the new SMPs could be tailored to near body temperature by varying BM content, providing bright prospect in biomedical applications in human body.[32,33]

The interfacial interaction between BM and PPSe was revealed by FTIR, XPS, and XRD measurements. The effects of BM content and curing extent on the performance, such as mechanical properties, biodegradability, and shape memory properties (switching temperature, shape recovery, and shape fixity), of the composites were investigated and correlated to the structure of PPSe/BM nanocomposites. The cell viability and attachment on the PPSe/BM composite substrates were conducted to examine their biocompatibility. In vitro degradation experiments in phosphate buffer saline (PBS) were performed to evaluate the biodegradability of the composites.

## EXPERIMENTAL SECTION

**Raw Materials.** PDO (98.0%), SA (99.9%), and IA (99.0%) were purchased from Hunan Rivers Bioengineering Co. Ltd., Tianjin Damao Chemicals, and Qingdao Kehai Biochemistry Co. Ltd., respectively. BM was purchased from Shandong Aluminum Co. Ltd. The diol and diacids were used as received. BM was dried in vacuo before use. Tetra-*n*-butyl titanate (TBT, 98%), *p*-hydroxyanisole, and analytic grade dicumyl peroxide (DCP) were obtained from SinoPharm Group and the latter two were purified by recrystallization before use.

**Synthesis of PPSe and Preparation of SMPs.** PPSe with diol/diacids mole ratio of 1.05 and SA/IA molar ratio of 9 was synthesized by melt polycondensation according to the previous report.[26] The synthesized PPSe was purified via dissolving in chloroform and precipitating in cold methanol repeatedly. The number average molecular weight and polydispersity index ($M_w/M_n$) of PPSe were examined by gel permeation chromatography (GPC), about 30000−40000 g/mol and 2.00−4.89, respectively.

For the preparation of SMPs, PPSe, BM, and DCP were mixed on a two-roll open mill and then compression molded at 150 °C for 15 min. They could be completely cured via this process according to the gel fraction determination.[26] The compounds of PPSe and BM were named as PPSe/BM composites. The sample code of PPSe-B10 symbolizes PPSe/BM composites with 10 phr of BM per 100 phr of PPSe. The others can be deduced by analogy.

**Measurements.** The molecular weight and its distribution were measured by GPC using tetrahydrofuran as the solvent (GPC, Agilent 1100, with Waters 2415 as the detector and Waters 515 as the pump), in which a nonpolar polystyrene gel stationary phase was used. Calibration curve of PPSe was obtained by using polystyrene standard and universal calibration methods. The average molecular weight and polydispersity index ($M_w/M_n$) of the PPSe used in our experiments were uniform, which were about 26616 g/mol and 2.09, respectively. The X-ray photoelectron spectroscopy (XPS) spectra of BM and m-BM were recorded by using an X-ray Photoelectron Spectrometer (Kratos Axis Ultra DLD) with an aluminum (mono) K$\alpha$ source (1486.6 eV). The aluminum K$\alpha$ source was operated at 15 kV and 10 mA. For both samples, a high-resolution survey (pass energy is equal to 48 eV) was performed at spectral regions relating to aluminum atoms. All core level spectra were referenced to the C1s neutral carbon peak at 284.6 eV. Fourier transform infrared spectroscopy (FTIR) was performed on a Bio-Rad 165 Fourier transform infrared spectrophotometer (Bio-Rad Laboratories, Hercules, CA) with the samples in KBr pellets. The X-ray diffraction (XRD) studies were conducted at ambient temperature on a Rigaku Dmax/III diffractometer using $CuK_\alpha$ radiation ($\lambda$ = 1.54 Å). Accelerating voltage and current were 40 kV and 30 mA, respectively. All the samples were scanned from 5° to 60° with a step length of 0.02° at 24 °C.

Melting and crystallization of PPSe/BM composites with variable DCP content were determined with differential scanning calorimetry (DSC) on a TA Q20 machine (USA). The thermal history of the samples was eliminated by heating them to 150 °C. The samples were then cooled to −65 °C and reheated at 10 °C/min to measure the $T_m$. The cryogenically fractured surfaces of the nanocomposites were observed with an EVO 18 Scanning Eletron Microscope (Germany). High resolution transmission electron microscopy (HRTEM) was conducted on a JEOL2100 TEM machine. The tensile tests above $T_m$ were performed by using a TA DMA Q800 machine. After equilibrating at $T_m$ + 10 °C for 10 min, the samples were stretched at 0.1 N/min until fracture. The tensile tests at elevated temperature were repeated for at least three times. Dynamic mechanical analysis (DMA) was conducted with an EPLEXOR 500N DMTS instrument (GABO, Germany) under a tensile mode with dynamic strain of 0.5%. The frequency and heating rate were set as 1 Hz and 3 °C/min, respectively.

The thermomechanical cycle experiments were also performed with a TA DMA Q800 machine to characterize the shape memory behavior of PPSe/BM composites. Prior to deformation, the samples (20.0 mm ×5.0 mm ×0.7 mm) were heated to $T_m$ + 20 °C and equilibrated for 10 min. In step 1, the samples were deformed by ramping force from preloaded 0.005N to a designed value at a rate of 0.1 N/min (0.05 N/min for the neat PPSe) (deformation). In step 2, the samples were cooled at a rate of 3 °C/min to $T_m$ − 20 °C under constant force to fix the deformation (cooling). In step 3, the force exerted on the samples was unloaded to the preloaded value (0.005 N) at the rate of 0.1 N/min (0.05 N/min for the neat PPSe), followed by an additional 10 min of isothermal step to ensure shape fixing at $T_m$ − 30 °C (unloading and shape fixing). In the final step, the samples were reheated at the rate of 3 °C/min to $T_m$ + 20 °C and then held for 10 min to recover any possible residual strain (recovery). The thermomechanical cycle consisting of the four steps above was repeated three times for each sample. Upon unloading, part of the strain ($\varepsilon_m - \varepsilon_u$) was instantaneously recovered, leaving an unloading strain ($\varepsilon_u$). The recovery process left a permanent strain ($\varepsilon_{p(N)}$). Shape fixity (SF) and shape recovery (SR) are defined as below.

$$\mathrm{SF}(\%) = \frac{\varepsilon_u}{\varepsilon_m} \times 100,\ \ \mathrm{SR}(\%) = \frac{\varepsilon_m - \varepsilon_{p(N)}}{\varepsilon_m - \varepsilon_{p(N-1)}} \times 100$$

In vitro cell response on the composites was performed. The specimens with 1 mm thickness were cultured in PBS for 8 h to minish the effects of impurity on cells, sterilized via washing with ethanol solution in sterilized water (75 vol %) and exposure to Co60 for 15 min, and afterward incubated in Dulbecco's modified Eagle's medium (DMEM) of 3 $cm^2$/ml at 37 °C for 24 h. The extract was filtrated (0.22 mm pore size) to get rid of the solid particles of the material. The liquor after degradation was filtered (0.22 mm pore size) to remove the bacterium and impurity from the liquid. L929 cells were cultured in DMEM added to 10 vol % fetal bovine serum (FBS) at a seeding density of 4.0 × $10^4$ cells/ml, and then plated onto 96-well micrometer plates. The cells were cultured in a moist atmosphere with 95% air and 5% $CO_2$ at 37 °C for 24 h. Subsequently, the culture medium was substituted by the extract dilutions (50 vol%), with the original medium regarded as the negative control.

MTT, a tetrazolium salt, could be adhered to a dark blue product by mitochondrial dehydrogenases in living rather than dead cells.[34] After being cultured for 1, 2, and 3 d, the cells were dyed with MTT at 50 mL/well (MTT in medium 199 without phenol red, 5 mg/mL, Sigma, St. Louis, USA), and further incubated for 4 h at 37 °C under the same condition. Thereafter MTT was removed and 100 mL/well of isopropanol (BDH, Poole, England) was put in to dissolve the formazan crystals. The optical density (OD) value could be revealed on a multiwell microplate reader (EL 312e Biokinetics reader, Biotek Instruments) at 570 nm. All material extracts were subjected to at least three separate experiments, providing comparable results. After being cultured for 1, 2, and 3 d, and before the MTT testing, the growing morphology of L929 cells in the negative control and the extract substrates was observed utilizing an inverted phase contrast microscope (OLYMPUS IX50-S8F2).

In vitro degradation of the composites was done in PBS. A proper solution-to-mass ratio, 50:1, was employed, that is, 10 mL of PBS solution for one sample with average mass of 0.2 g. Ten slabs for each sample were immersed in PBS solution with pH of 7.4 at 37 °C in a shaking water bath with a rotation speed of 20 rpm. Over the course of study, the pH values of the PBS were closely monitored. The PBS solution was changed fresh every five days. The samples were removed at different time points, dried at 40 °C, and weighted. Dry weight changes were thus determined.

## RESULTS AND DISCUSSION

**Effects of BM on the Structure and Properties of PPSe.** As pure PPSe has poor strength above $T_m$, with tensile strength less than 1 MPa, which may restrict some kinds of applications as biomedical materials, enhancement of rubbery modulus of PPSe is especially important in many circumstances. Herein, we expected to employ BM as reinforcement to strengthen PPSe. Being terminated with hydroxyl and carboxyl, PPSe is in all probability to have well compatibility with BM, which owns large amounts of surface aluminols. As a matter of fact, enough characterization approaches were constructed to fully demonstrate the interface interaction between PPSe and BM, including FTIR, XPS (Supporting Information), and XRD measurements. The results proved that the terminal carboxyl and hydroxyl groups of PPSe reacted with the hydroxyls on the surface of BM well. Therefore, BM could be uniformly dispersed in PPSe matrix and enhance the rubber modulus of PPSe effectively.

Figure 1 reveals SEM and TEM observations of PPSe/BM composites. It can be seen that BM nanoplatelets were well

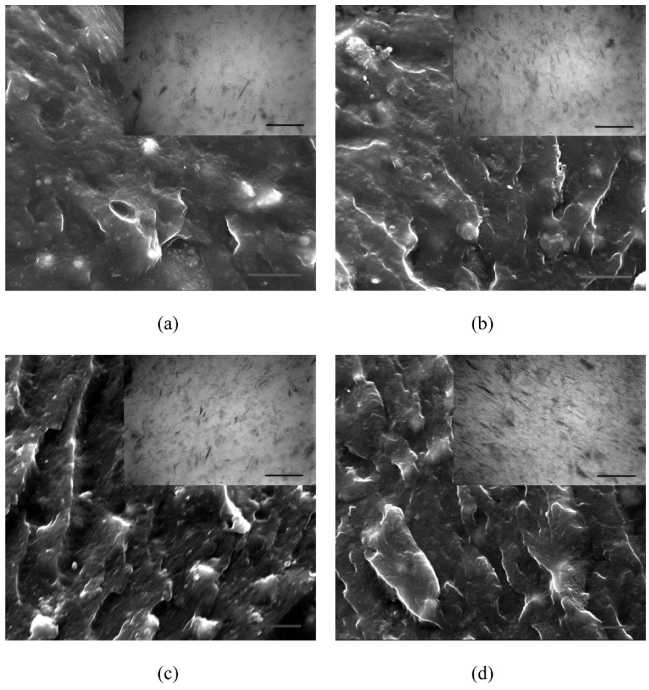


**Figure 1.** SEM and TEM photos of PPSe/BM composites. (a) PPSe-B10, (b) PPSe-B20, (c) PPSe-B30, and (d) PPSe-B40. The scale bars in the SEM and TEM photos are 200 nm and 10 $\mu$m, respectively.

dispersed in the polyester matrix at lower BM content (not more than 30 phr) which indicated that BM had good compatibility with PPSe. Some aggregations were observed in the SEM and TEM images of the composites with BM content of 40 phr, as shown in Figure 1d. The uniform dispersion of BM in PPSe should be due to the substantiated strong interface interactions between PPSe and BM.

The well dispersion of BM nanoparticals in PPSe stands to reason that PPSe/BM composites have enhanced strength in rubbery state. Figure 2 shows the dependence of the mechanical properties of PPSe/BM nanocomposites above $T_m$ on BM content. It is clearly revealed that the overall mechanical properties significantly increased with increasing BM loading. The tensile stress above Tm increased dramatically. For example, with 40 phr of BM loading, the tensile strength increased from 0.8 to 2.9 MPa, showing 263% increment compared to pure PPSe. The elongation at break of all composites did not change a lot. This is due to that BM reacted with PPSe chains and acted as cross-linking points.

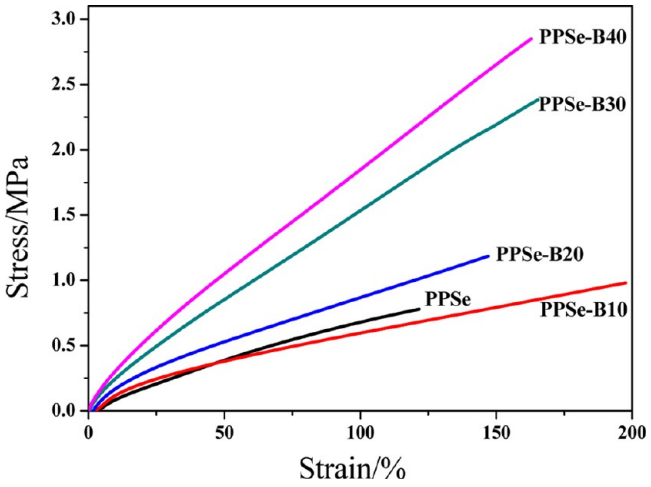


**Figure 2.** Tensile stress−strain curves of the composites at elevated temperature ($T_m$ + 10 °C). The samples were cured by 0.5 phr of DCP.

Then, the interaction between the interfaces of BM and PPSe was enhanced and the dispersibility of BM improved. Meanwhile, the amount of cross-linking points increased with increasing BM content, which resulted in higher Young's modulus at elevated temperature and slightly improved elongation at break for the system with higher BM content. The substantially increased mechanical properties of the PPSe/BM nanocomposites could be attributed to the excellent dispersion of BM facilitated by the interactions between BM and PPSe, and the compatibility between BM and PPSe.

Figure 3 depicts dynamic mechanical analysis curves of PPSe/BM nanocomposites. All the samples presented glass

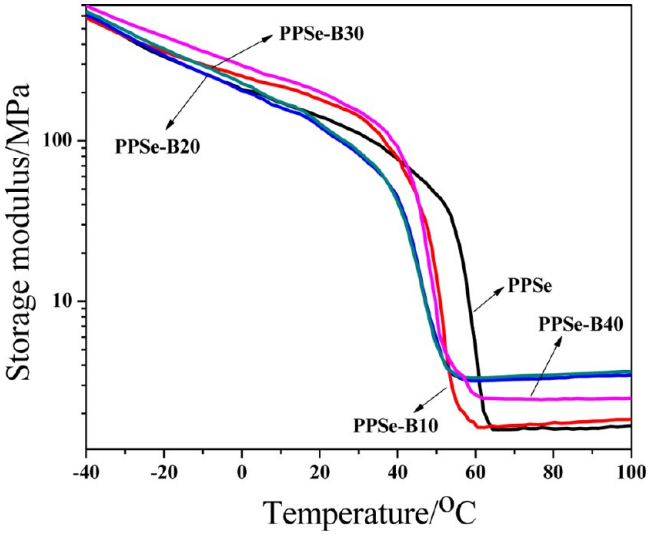


**Figure 3.** Storage modulus of PPSe/BM composites with different BM contents (cured by 0.5 phr of DCP).

state at low temperature and rubbery state with lower modulus E′ at high temperature of a wide range. The drop of $E'$ was due to the glass transition of amorphous phase and the melting of crystallization phase of the composites.[35,36] All the samples had high storage modulus ratios of over 100 ($E'_{low} > 100E'_{high}$) and high modulus at the scale of $10^6$ Pa at high temperature. The high ratio of storage modulus below $T_m$ to that above $T_m$ is preferred for SMPs and an essential requirement for shape memory applications,[7,37] via benefiting the deformation at high temperature and the fixing of temporary shape at low temperature.[35] As shown, storage modulus $E'$ of the composites had certain improvement when BM was incorporated. When BM particles content was not more than 30 phr, BM could be dispersed uniformly in the polyester matrix and acted as cross-linking points, resulting in distinct increase trend in rubbery modulus of the composites. With increasing BM content of 40 phr, some aggregations were observed as shown in Figure 1d. The aggregations were stress concentration points, which led to the decrease of the rubbery modulus. The high storage modulus in rubbery state could result in larger stress reservation of deformation while cooling, which would be favorable for shape recovery.[36] For the samples with higher storage modulus in rubbery state, more deforming energy was needed at $T_{deformation}$ and more energy was stored with the loss of elastic entropy when the samples were cooled down to $T_{fixing}$. As a result, the samples with higher storage modulus above $T_m$ had higher tendency and larger recovery stress to return to their original shapes, which meant faster shape recovery speed. Thus, the higher storage modulus above $T_m$ of PPSe/BM composites indicated the recovery stress of the SMPs was large enough for some applications with constraint environments.[35]

The introduction of BM might substantially change the crystallization of PPSe/BM composites, which was illustrated in the XRD spectra of Figure 4a. Both uncured and cured composites showed peaks at $\theta$ = 28.1°, 38.4°, and 49.2°, which were assigned to BM. This illustrated that most octahedral structures of BM were not destroyed in PPSe/BM composites. The presence of BM nanoplatelets restricted the crystallization of PPSe significantly. For cured PPSe-B40 composites, the characteristic peaks of PPSe at $\theta$ = 18−25° almost disappeared and the crystallization configuration changed entirely. The result provided additional hints for the possible interaction between the surface aluminum hydroxyls of BM and the terminal carboxyl groups of PPSe during the processing of the composites. Figure 4b showed the crystallization enthalpy and crystallization temperature of PPSe/BM composites with variable BM content. With increasing BM loading, the crystallization enthalpy decreased first and then increased, which could be explained as follows. When a small quantity of BM was loaded, it affected little on the crystallization behavior of PPSe. With 30 phr of BM loading, it had enough impact on the crystallization behavior of PPSe, and decreased the crystallization enthalpy of PPSe to a great extent. When 40 phr of BM was introduced, aggregation of BM alleviated the restricting effect of BM on the crystallization behavior of PPSe. Thus the crystallization enthalpy of PPSe increased again. Meanwhile, with increasing BM content, the crystallization temperature decreased consistently from 15.3 to 7.8 °C. The results stated BM did affect the crystallization behavior of PPSe remarkably.

**Shape Memory Behavior of PPSe/BM Composites.** For semicrystalline polyester composites, their shape memory behavior could be tailored via crystallization and melting of the composites. With changing $T_m$ of the composites, the transition temperature of the system changed accordingly. In this study, both cross-linking degree and BM content could limit crystallization and $T_m$ of PPSe/BM composites to an extent. Figure 5 describes dependences of $T_m$ of PPSe/BM composites on BM and DCP content. BM and DCP content in the composites were in the ranges of 0−40 wt % and 0−0.8 wt

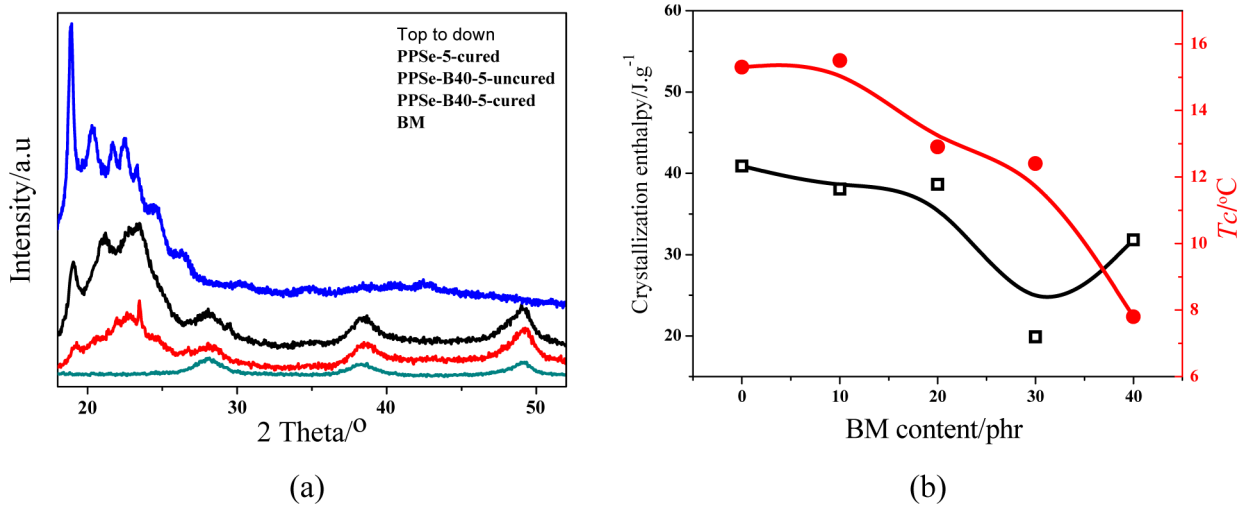


**Figure 4.** Effects of BM on the crystallization of PPSe: (a) WAXD pattern and (b) evolutions of crystallization enthalpy and crystallization temperature (cured by 0.5 phr of DCP).

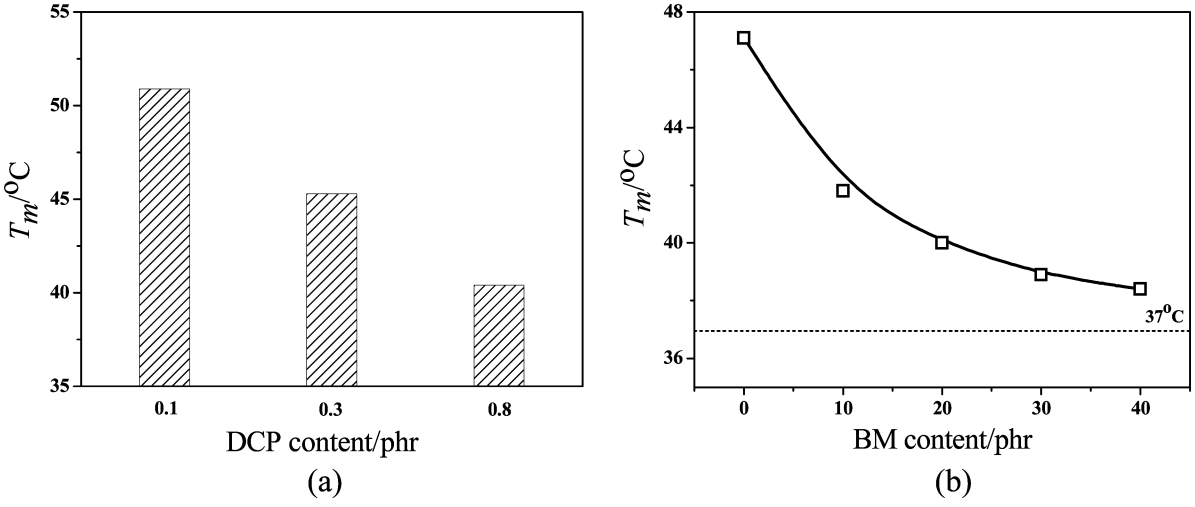


**Figure 5.** Effects of DCP content (a) and BM content (b) on $T_m$ of PPSe/BM composites (BM content of the samples in (a) was 10 phr; the samples in b were cured by 0.5 phr of DCP).

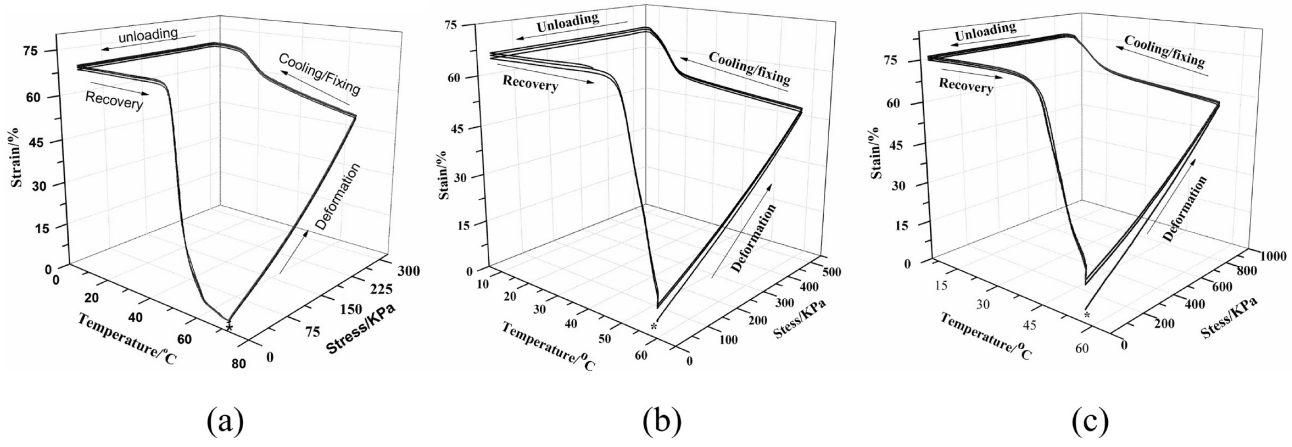


**Figure 6.** 3D diagram of stress-controlled programming cycles for (a) PPSe, (b) PPSe-B20, and (c) PPSe-B40. All the samples were cured with 0.5 phr of DCP.

% (relative to PPSe), respectively. Through changing composition and cross-linking degree, $T_m$ of the composites decreased from 50.6 to 38.5 °C.

With increasing DCP content, $T_m$ of the composites decreased continuously. The cross-linking of the composites restrained the crystallization process. The cross-links sup-

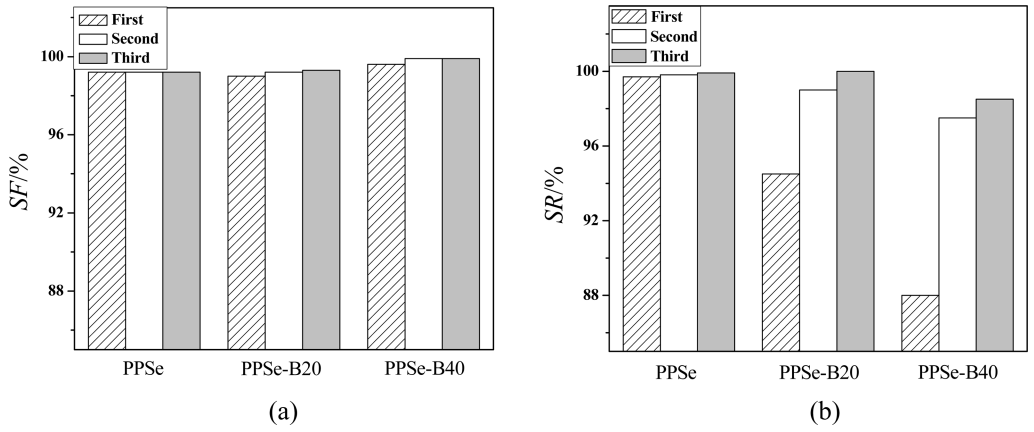


**Figure 7.** SF and SR values of PPSe/BM composites (cured by 0.5 phr of DCP).

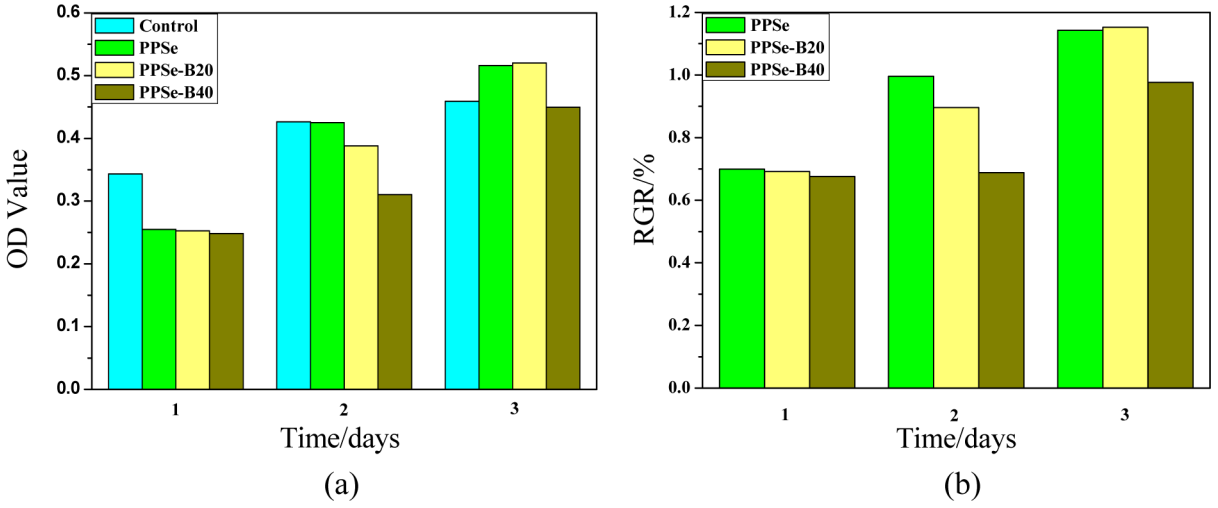


**Figure 8.** Optical density (OD) value (a) and relative growth rate (RGR/%) (b) of L929 cells cultured on PPSe/BM composites with different content of BM compared with that on control substrate.

pressed chain mobility and the ordering of segments into lattices, which therefore decreased the size of crystallite and lowered $T_m$. The effect of BM content on $T_m$ was similar to that of DCP, both of which made the composites crystallize in less perfection and thus have lower $T_m$. Because of the reaction with terminal carboxyl groups of PPSe or the physically interaction with PPSe, BM limited the movements of the chains of PPSe and the crystallization behavior of the composites was suppressed to an extent. That is to say, BM restrained the chain mobility via acting as cross-linking points rather than produced heterogeneous nucleation in the course of crystallization. From Figure 5b, we can find $T_m$, that is, the transformation temperature of the shape memory composites could be tailored near body temperature via changing their compositions and curing contents. If the transformation temperature of the SMPs was near or a little above body temperature, they would have well potential biomedical applications in body.[32,33] The present results demonstrated the perspectives of PPSe/BM in biomedical devices used in vivo.

The cyclic stress-controlled behavior of pure PPSe and PPSe/BM composites is shown in Figure 6 for the first three thernomechnical cycles, and the shape fixity (SF) and shape recovery (SR) values are summarized in Figure 7. We can see the PPSe/BM composites maintained excellent shape memory properties of PPSe which have been demonstrated previously.[26]

Figure 7a shows SF of all samples was over 99% and increased with BM content. Compared the PPSe/BM composites with pure PPSe, the BM nanoplatelets incorporated into the PPSe matrix suppressed the movements of polymer chains, retarded the creep of the polymer chains, and made them move quite slowly under constant force. Therefore, retraction of the chains during the stretching and cooling of PPSe-B20 and PPSe-B40 were less complete than that of pure PPSe. When the force was removed, the chains of PPSe-B20 and PPSe-B40 were still in the stretching state, resulting in slightly larger SF. Figure 7b depicts the effects of BM content on the SR values of PPSe/BM composites, which decreased with BM content in the first cycle. However, the SR values of PPSe/BM composites increased to the value close to that of PPSe, and kept well in the followed cycles. Ideally, together with high SF, SR of the composites should increase with increasing BM content. On the one hand, for PPSe-B20 and PPSe-B40, the polymer chains remained stretched after loading and cooling, which could induce large recovery upon reheating driven by the entropy elasticity. On the other hand, high rubbery modulus of the material also favored higher SR.[37] BM nanoplatelets showed dual effects of reinforcement and multifunctional cross-linkers, improving rubbery modulus of

the composites greatly. Therefore high BM content should bring in high SR. Nevertheless, the obtained result did not correspond with the case. This unexpected result was due to that all BM added could not act as cross-linkers. Excess BM (not chemically bonded with PPSe chain) tends to aggregate, which would be detrimental to the elasticity of the composites. Besides, polymer chains and BM would slip against each other during stretching, resulting in deformation that could not restore. The two aspects above were both disadvantageous for shape recovery. With increasing BM content, these effects were more significant. Therefore, as BM content increased, SR of the system decreased but kept on a relatively good level. However, SR of PPSe/BM composites could be recovered to high value (close to that of PPSe) by increasing the cycle times. Such observation was due to that the rearrangement of the fillers occurred during the course of thermal mechanical cycles. Thus, the possibility of slipping between BM and the chains of PPSe decreased with increasing cycle times, which benefited shape recovery. In other studies, it was also proposed that fillers would be rearranged in the stretching direction during stretching.[38]

**Cell Viability and In Vitro Degradation of PPSe/BM Composites.** L929 cells were used as reference cells to evaluate the potential biocompatibility of PPSe/BM composites. The cell viability was estimated via MTT assay in accordance with the GB/T16175−1996 standard. Figure 8 shows the viability of the seeded cells on the various substrates for 1, 2, and 3 days compared with those on control substrates. The OD value of a material accounts for the growth situation of the cells incubated on the extract substrates. The larger the OD value is, the better the cells grow. From Figure 8a, we can see, the OD value of the cells incubated on the composite substrates increased with time and even outnumbered that on the control substrate, which means the cell number increased obviously. The RGR value is calculated according to the formula as below.

$$\mathrm{RGR}/\% = \frac{\text{absorbance of the material} - \text{absorbance of the blank}}{\text{absorbance of the negative} - \text{absorbance of the blank}} \times 100$$

On the basis of GB/T16175−1996 standard, the cytotoxicity of materials with different RGR values is classified to six grades as shown in the Supporting Information (Table S1). Grade 0 and 1 are qualified to be noncytotoxic. Grade 2 should be further appraised by considering the cell's morphology. The other grades are considered to be unqualified. We can find all the RGR values of the cells cultured on the composite substrates for 3 days were above 95% and belonged to grade 1 or 0, even though some were corresponding to grade 2 before. Therefore it is concluded that PPSe/BM composites show no toxicity on the cell viability.

Figure 9 shows the photomicrographs of the L929 cells incubated for 3days in the negative control and the extract substrates of PPSe/BM composites. All the cells were in well growing condition and overspreaded on the culture substrates. The growthform of the cells in the extract substrates of PPSe/BM composites were similar to those in negative control, suggesting no cytotoxicity and potential biocompatibility of PPSe/BM composites.

The relatively easy degradation in PBS at 37 °C of the SMPs was reported previously.[26] However, it cannot meet the requirement of faster degradation which is essential for some

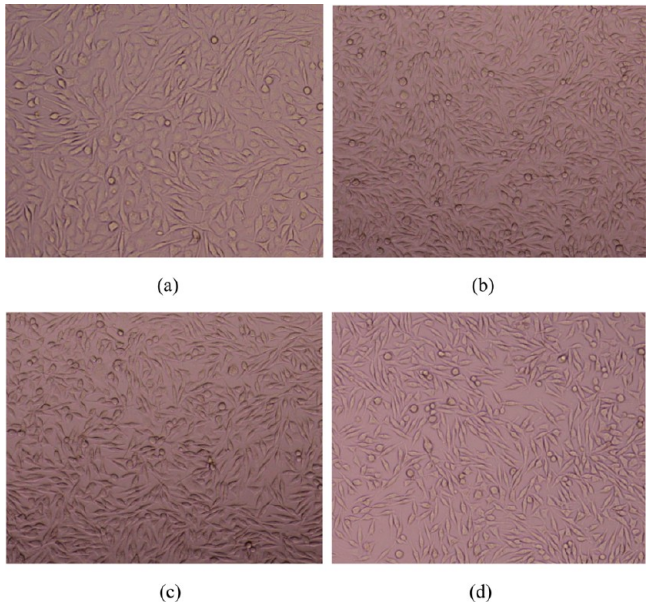


**Figure 9.** Photomicrographs of the L929 cells incubated for 3days in the negative control (a) and the extract substrates of PPSe/BM composites (b−d). (b, pure PPSe; c, PPSe-B20; d, PPSe-B40).

in vivo applications. Figure 10 depicts the weight loss evolution of PPSe/BM Composites in PBS up to over 2 months. It can be

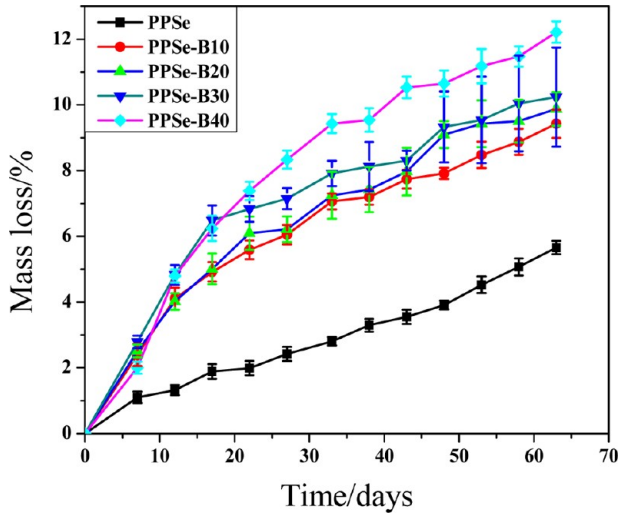


**Figure 10.** Weight loss of PPSe/BM composites in PBS at 37 °C, as a function of time.

seen that all of the composites lost their weight in PBS gradually, and the introduction of BM accelerated degradation of the PPSe/BM composites substantially compared to pure PPSe. The degradation rate of the composites increased gradually with increasing BM loading. Especially for PPSe-BM40, the mass loss was twice as much as pure PPSe when degraded in PBS for 2 months.

There are several factors for the faster degradation rate of PPSe/BM composites compared to neat PPSe. First, the degradation reaction of the polyester is reversible. When ester linkages in PPSe were randomly cleaved via hydrolysis, the degradation of PBS would be slowed down due to the accumulation of the acidic degradation products. Consequently, due to the basicity endowed by the surface aluminols, BM

might increase the pH value of PBS by neutralizing the degradation products of PPSe, resulting in higher degradation rate of the PPSe/BM composites. Some early reports had similar results.[20,39] Second, the BM nanoplatelets with excellent hydrophilicity favored the infiltration of PBS into the composites and thus promoted their degradation. Yu et al.[20] had similar viewpoint in the report of $\varepsilon$-PCL/$Fe_3O_4$ system. Third, it is well-known that the hydrolysis of semicrystalline polyester is highly dependent on the crystallinity. The higher the crystallinity is, the lower mass loss rate the polyester possesses. As we know above that with increasing BM loading, the chain mobility of PPSe was suppressed and the crystallization was restrained gradually. Thus, the crystallinity decreased successively from PPSe-B10 to PPSe-B40 with increasing BM content. At the same time, as $T_m$ of the composites depressed with increasing BM loading, $T_m$ of PPSe-B40 was the closest to 37 °C, which was also favorable for its degradation in PBS of 37 °C. As a consequence, the degradation rate of the PPSe/BM composites increased with increasing BM loading. Finally, with increasing BM content, some of the BM acting as fillers alone did not link with PPSe chains. Thus, when the composites degraded, this part of BM broke off from the surface, increasing the apparent degradation rate of the PPSe/BM composites as a whole.

In soft tissue engineering applications, flexible but relatively tough materials that degrade in accordance with the rate of tissue regeneration are required.[40,41] Herein, the faster and tunable biodegradation rate of the PPSe/BM composites makes them more promising for such kinds of biomedical applications.

## CONCLUSION

Aiming at stronger and faster degradable shape memory polymers, boehmite nanoplatelets were introduced into poly(propylene sebacate) which has been synthesized with fully biobased raw materials. By varying the BM content and curing extent, the transformation temperature of SMPs based on PPSe/BM composites could be tuned to be close to body temperature. The interactions between BM and PPSe chain, which are essential for the compatibility between them, were characterized in detail. Because of the uniform dispersion of BM and the interfacial interactions, the mechanical properties of PPSe above $T_m$, including strength and modulus, were increased significantly. The excellent SF and SR of PPSe based SMP were maintained in the PPSe/BM composites. The PPSe/BM composites showed no toxicity toward L929 cells in view of the viability data and excellent cell attachment. Remarkably increased degradation rate was realized in PPSe/BM composites, compared with that of the neat PPSe. Several interesting characteristics, such as high mechanical properties, excellent shape memory (with transformation temperature close to body temperature) and potentially biocompatibility, make the SMPs based on PPSe/BM composites good candidates to be used as biomedical materials, such as high strength stents, hard tissue implantations or short-term clinical outcomes in which fast degradation rate is necessary.

## ASSOCIATED CONTENT

### Supporting Information

Preparation of m-BM Model Compounds, XPS spectra of BM and m-BM, FTIR spectra of BM, PPSe, m-BM, uncured and cured PPSe/BM composites, and the standard of the response grades for cytotoxicity. This material is available free of charge via the Internet at http://pubs.acs.org/.

## AUTHOR INFORMATION

### Corresponding Author

*Tel: +86 20 87113374 (B.C.G.); +86 10 64421186 (L.Q.Z.). Fax: +86 20 22236688 (B.C.G.); +86 10 64421186 (L.Q.Z.). E-mail: psbcguo@scut.edu.cn (B.C.G.); zhanglq@mail.buct.edu.cn (L.Q.Z.).

### Notes

The authors declare no competing financial interest.

## ACKNOWLEDGMENTS

This work was supported by National Natural Science Foundation of China (50933001), Program for New Century Excellent Talents in University (NCET-10-0393) and Fundamental Research Project for the Central Universities (2012ZG0002).

## REFERENCES

(1) Liu, C.; Qin, H.; Mather, P. T. *J. Mater. Chem.* **2007**, *17*, 1543.
(2) Lendlein, A.; Jiang, H.; Jünger, O.; Langer, R. *Nature* **2005**, *434*, 879.
(3) Huang, W.; Yang, B.; An, L.; Li, C.; Chan, Y. *Appl. Phys. Lett.* **2005**, *86*, 114105.
(4) Luo, X.; Mather, P. T. *Soft Matter* **2010**, *6*, 2146.
(5) Mohr, R.; Kratz, K.; Weigel, T.; Lucka-Gabor, M.; Moneke, M.; Lendlein, A. *Proc. Natl. Acad. Sci. U.S.A.* **2006**, *103*, 3540.
(6) Leng, J.; Lan, X.; Liu, Y.; Du, S. *Prog. Mater. Sci.* **2011**, *56*, 1077.
(7) Pan, Y.; Liu, T.; Li, J.; Zheng, Z.; Ding, X.; Peng, Y. *J. Polym. Sci., Part B: Polym. Phys.* **2011**, *49*, 1241.
(8) De Groot K, D. P. C.; Smitt, P; Driessen, A. *Sci. Ceram.* **1981**, *11*, 433.
(9) Filion, T. M.; Xu, J.; Prasad, M. L.; Song, J. *Biomaterials* **2011**, *32*, 985.
(10) Gunes, I. S.; Jimenez, G. A.; Jana, S. C. *Carbon* **2009**, *47*, 981.
(11) Xiao, Y.; Zhou, S.; Wang, L.; Gong, T. *ACS Appl. Mater. Interfaces* **2010**, *2*, 3506.
(12) Koerner, H.; Price, G.; Pearce, N. A.; Alexander, M.; Vaia, R. A. *Nat. Mater.* **2004**, *3*, 115.
(13) Dawei, Z.; Yanju, L.; Jinsong, L. *Proc. SPIE* **2008**, 6932.
(14) Cho, J. W.; Kim, J. W.; Jung, Y. C.; Goo, N. S. *Macromol. Rapid Commun.* **2005**, *26*, 412.
(15) Lee, H. F.; Yu, H. H. *Soft Matter* **2011**, *7*, 3801.
(16) Lendlein, A.; Zotzmann, J.; Feng, Y.; Alteheld, A.; Kelch, S. *Biomacromolecules* **2009**, *10*, 975.
(17) Bertmer, M.; Buda, A.; Blomenkamp-Höfges, I.; Kelch, S.; Lendlein, A. *Macromolecules* **2005**, *38*, 3793.
(18) Lendlein, A.; Kelch, S. *Clin. Hemorheol. Microcirc.* **2005**, *32*, 105.
(19) Lendlein, A.; Langer, R. *Science* **2002**, *296*, 1673.
(20) Yu, X.; Zhou, S.; Zheng, X.; Xiao, Y.; Guo, T. *J. Phys. Chem. C* **2009**, *113*, 17630.
(21) Huang, F.-L.; Dai, H.-L.; Fang, Y.; Shan, X.-Z.; Li, S.-P. *J. Inorg. Mater.* **2007**, *22*, 333.
(22) Guo, X. D.; Zheng, Q. X.; Du, J. Y.; Quan, D. P.; Yan, Y. H.; Li, S. P. *J. Wuhan Univ. Technol., Mater. Sci. Ed.* **1998**, *13*, 9.
(23) Knight, P. T.; Lee, K. M.; Chung, T.; Mather, P. T. *Macromolecules* **2009**, *42*, 6596.
(24) Nijst, C. L. E.; Bruggeman, J. P.; Karp, J. M.; Ferreira, L.; Zumbuehl, A.; Bettinger, C. J.; Langer, R. *Biomacromolecules* **2007**, *8*, 3067.
(25) Zhang, D. W.; Leng, J. S.; Liu, Y. J. *Adv. Mater. Res.* **2008**, *47*, 690.
(26) Guo, B.; Chen, Y.; Lei, Y.; Zhang, L.; Zhou, W. Y.; Rabie, A. B. M.; Zhao, J. *Biomacromolecules* **2011**, *12*, 1312.
(27) Kuang, D.; Fang, Y.; Liu, H.; Frommen, C.; Fenske, D. *J. Mater. Chem.* **2003**, *13*, 660.
(28) Raybaud, P.; Digne, M.; Iftimie, R.; Wellens, W.; Euzen, P.; Toulhoat, H. *J. Catal.* **2001**, *201*, 236.

(29) Hemingway, B. S.; Robie, R. A.; Apps, J. A. *American Mineral.* **1991**, *76*, 445.
(30) Chen, W.; Wu, S.; Lei, Y.; Liao, Z.; Guo, B.; Liang, X.; Jia, D. *Polymer* **2011**, *52*, 4387.
(31) Wang, M. S.; Pinnavaia, T. J. *Chem. Mater.* **1994**, *6*, 468.
(32) Xue, L.; Dai, S.; Li, Z. *Macromolecules* **2009**, *42*, 964.
(33) Li, Y. G.; Wang, Y. L.; Luo, Y. F. *Adv. Mater. Res.* **2009**, *79*, 271.
(34) Mosmann, T. *J. Immunol. Methods* **1983**, *65*, 55.
(35) Xu, J.; Shi, W.; Pang, W. *Polymer* **2006**, *47*, 457.
(36) Chun, B. C.; Cho, T. K.; Chong, M. H.; Chung, Y. C. *J. Mater. Sci.* **2007**, *42*, 9045.
(37) Jung, D.; Jeong, H.; Kim, B. *J. Mater. Chem.* **2010**, *20*, 3458.
(38) Hu, J. W.; Li, M. W.; Zhang, M. Q.; Xiao, D. S.; Cheng, G. S.; Rong, M. Z. *Macromol. Rapid Commun.* **2003**, *24*, 889.
(39) Zheng, X.; Zhou, S.; Yu, X.; Li, X.; Feng, B.; Qu, S.; Weng, J. *J. Biomed. Mater. Res., Part B* **2008**, *86B*, 170.
(40) Niklason, L.; Gao, J.; Abbott, W.; Hirschi, K.; Houser, S.; Marini, R.; Langer, R. *Science* **1999**, *284*, 489.
(41) den Dunnen, W. F. A.; Meek, M. F.; Grijpma, D. W.; Robinson, P. F.; Schakenraad, J. M *J. Biomed. Mater. Res.* **2000**, *51*, 575.